Thermal Signatures of the Kondo Volume Collapse in Cerium

M. J. Lipp, D. Jackson, H. Cynn, C. Aracne, W. J. Evans, and A. K. McMahan

H-Division, Physical Sciences, Lawrence Livermore National Laboratory, Livermore, California 94550, USA

(Received 10 June 2008; revised manuscript received 6 August 2008; published 15 October 2008)

X-ray diffraction measurements of cerium in the vicinity of the isostructural γ-α transition have been performed with high precision and accuracy from room temperature to almost 800 K. The disputed location of the critical point has been found to occur at 1.5 ± 0.1 GPa and 480 ± 10 K. The data are well fit by the Kondo volume collapse model plus a quasiharmonic representation of the phonons. The resultant free energy is validated against data for the thermodynamic Grüneisen parameter and, beyond the dominant spin-fluctuation contribution, indicates a dramatic change in the lattice Grüneisen parameter across the transition.

DOI: 10.1103/PhysRevLett.101.165703 PACS numbers: 64.70.K−, 62.50.−p, 64.30.Ef

Cerium continues to excite both theoretical and experimental work based on its unique behavior among the elements. One of its most fascinating features is found in its large isostructural (fcc) volume collapse (VC) under compression between the γ- and α-phase. Over the years a number of theoretical models have attempted to explain the underlying physics governing this volume collapse whose size decreases with increasing temperature and eventually terminates in a critical point (CP). Decades ago it was assumed that the transition was driven by valence changes, but inconsistencies with the cohesive energies of other lanthanides led to the conjecture that the VC was caused by a Mott transition in the $4f$ electrons [1]. This model continues to compete with the idea that the VC is caused by a dramatic change in Kondo screening of the local $4f$ moments [2–4], as borne out at least qualitatively by modern dynamical mean-field theory calculations [5–10]. The Kondo VC (KVC) model appears unique in predicting a second low-T critical point, which although inaccessible at negative pressure for Ce, has been observed in Ce alloys [11]. While the Mott and KVC scenarios focus on electronic effects, new experimental data indicate that nearly half the entropy change across the room-temperature (RT) transition is due to lattice vibrations, suggesting a closer examination of the role of phonons is required [12].

There appears to be a remarkable lack of modern high-quality pressure-volume (p-V) data for the Ce transition, especially at higher temperatures, which might be used to further constrain the considerable theoretical effort. Early pioneering work was either not performed by x-ray scattering techniques [13] or suffered from low signal-noise ratios [14]. Except for the x-ray study by Davis [14] all other older studies at higher temperature have relied on length measurements of macroscopic samples in large-volume presses. The results are often given as a plot of $(V - V_0)/V_0$ vs pressure neglecting changes of V_0 with temperature. Moreover, interpretation of the older data has led to several controversies, among them the location of the critical point [15,16] and the possibility that the VC continues as a second-order transition towards the melt line intersecting it close to the minimum or possibly more towards the phase boundary of the γ-, δ-phase and liquid [15,17].

The purpose of the current work was to provide a more substantial measurement of isotherms, with high-quality data obtained from energy dispersive as well as more precise angle dispersive x-ray diffraction (ADX), and with the temperature range previously considered extended by 200 K [18]. These results highly constrain the location of the CP. They provide no evidence of a second-order continuation of the transition, although a minimum in the bulk modulus does persist to the highest temperatures considered. While KVC modeling has generally only been in qualitative agreement with experiment, the present work also demonstrates that the functional forms of this model generate a quantitative fit to the data within experimental uncertainty. The inclusion of lattice vibrations is seen to be critical, and these results suggest a dramatic change in the lattice Grüneisen parameter across the transition.

For the experiments we employed diamond anvil cells (DAC) using anvils with 700 μm flats. Sample chambers were formed from steel gaskets indented to $\sim$100 μm thickness and holes of $\sim$200 μm diameter. All sample preparation was performed inside a glove box flushed with dry nitrogen or argon to inhibit oxide formation. Cerium chips were cut from ingots (Alfa Aesar, 99.8% nominal purity), smaller pieces pried off under a microscope and loaded with dry NaCl as pressure calibrant and transmitting medium. X-ray diffraction patterns were obtained at the beam-lines 16BMB and 16BMD (HPCAT) at the Advanced Photon Source (APS). Two-dimensional ADX images were recorded under compression, integrated using FIT2D [19] and analyzed. Temperature readings of the externally heated cells were taken by two thermocouples attached to opposing anvils and differed at most by 15 K.

With higher temperatures the patterns became increasingly spotty, possibly due to annealing and orientation

effects, which we attempted to mitigate using a larger diameter x-ray beam and oscillating the sample on its axis. Similar spottiness was observed at RT previously due to pressure-induced crystal grain growth associated with the transition from the fcc to the α-uranium structure at ~5 GPa [20].

Figure 1 shows selected p-V isotherms. Their close spacing on the higher volume side (see inset) indicates a small isobaric expansion coefficient. The RT data agree well with Jeong *et al.* [12] (99.99% purity), Schiwek *et al.* [18] (99.95%) and Olsen *et al.* [21] (99.9%). Below the CP the transition proceeds over an extended pressure range (see Fig. 2): At RT the transition started at 0.75 GPa and finished at 1.24 GPa (with 1.0 GPa as the halfway point), as observed before [21]. Our results clearly constrain the location of the CP characterized by $(\partial p/\partial V)_T = (\partial^2 p/\partial V^2)_T = 0$ and $(\partial^3 p/\partial V^3)_T < 0$ [22]. Using polynomial fits to each isotherm (not shown), only the fit to our data at 481 K is found to fulfill all three conditions. At lower temperatures we clearly observe a large-volume step and at higher temperatures the slope is no longer zero anywhere. The location of the CP has been in dispute for quite some time with the results spreading from 480 K and 1.45 GPa [16,23] to ~550 K and ~1.8 GPa [24,25] and even higher to ~640 K and ~2.05 GPa [13,26]. The most recent data place the CP at lower temperature again, namely, 485 K and 1.8 GPa [18]. Our results agree well with those of Kutsar [23] and Schiwek *et al.* [18]. A more detailed analysis of the previously published data based on the CP characterization [22], however, suggests a greater consensus since their pressure derivatives at temperatures higher than ~500 K [13,24] exceed zero, and/or hysteresis effects disappear [13,25] that can only exist below the CP [22]. Therefore all the apparently different locations for the CP are in fact all consistent and fall near 480 K and 1.5 GPa.

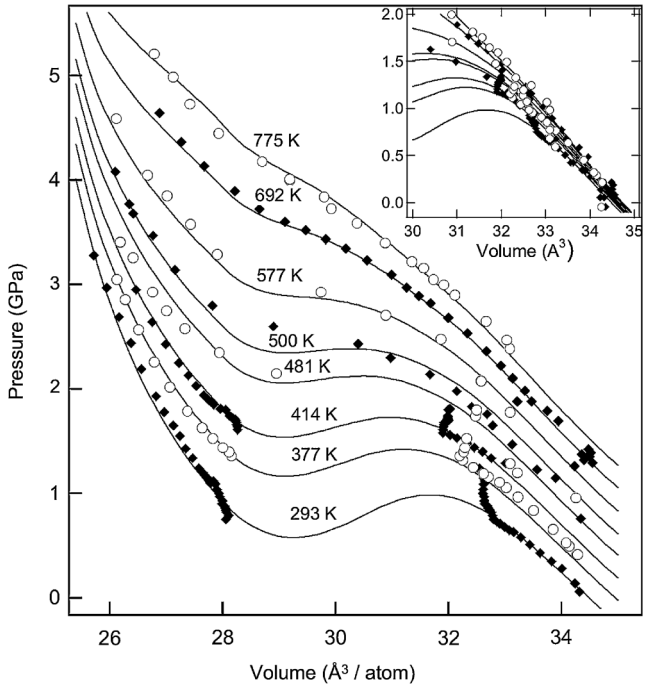

FIG. 1. Pressure-volume isotherms shifted by 0, 0.2, 0.4, ..., 1.4 GPa from lowest to highest for visual clarity. Pressures were determined using the NaCl equation of state [31]. The points are the present data, while the curves are functional forms of the KVC model (see text). The inset shows the unshifted results at large volume. Atomic volumes are accurate to about 0.05 Å^3, pressure uncertainty is estimated to be <0.05–0.1 GPa for data recorded using the same setup and x-ray calibration.

The curves in Fig. 1 show a fit to the present data obtained by the KVC model [2–4] as defined by the free energy per atom

$$F(V,T) = E_0(V) + k_B T(3\ln[\Theta(V)/T] - 1) + \int_0^T dT'(1 - T/T')C_{VK}(V,T'), \quad (1)$$

where the first term is the cold curve, the second a high-temperature quasiharmonic representation of the lattice vibrations, and the last the Kondo or spin-fluctuation contribution of the electrons. Debye function corrections to the lattice term are small for the present temperatures. Dynamical mean-field theory results [7] suggest that the additional charge excitation contribution from the electrons (the $\propto T$ term in C_V visible just above the Kondo peak) is small. We take $C_{VK}(V,T) = C_{VK}(T/T_K)$ [4] which is a peaked function, roughly symmetrical in $\ln(T/T_K)$, and characterized by ln(6) total entropy [27]. Parametrizations of the cold pressure $P_0(V)$, the lattice Grüneisen parameter $\gamma_{\rm lat}(V) = -d\ln\Theta(V)/d\ln V$, and the Kondo temperature $T_K(V)$ were used in fitting the experimental pressures to within a standard deviation of 0.08 GPa, comparable to experimental uncertainty.

Figure 3 shows the RT thermodynamic $\gamma = V(\partial P/\partial E)_V$ (solid curve, γ_1) and lattice $\gamma_{\rm lat}$ (dashed curve, $\gamma_{1,\rm lat}$) Grüneisen parameters as obtained from Eq. (1) using the parameters extracted from the pressure fit in Fig. 1. There is reasonable agreement between γ_1 and experiment given the scatter in the data. The dominant Kondo or electronic contribution to γ is localized within and near the two-phase region in Fig. 1, so that γ_1 and $\gamma_{1,\rm lat}$ are seen to

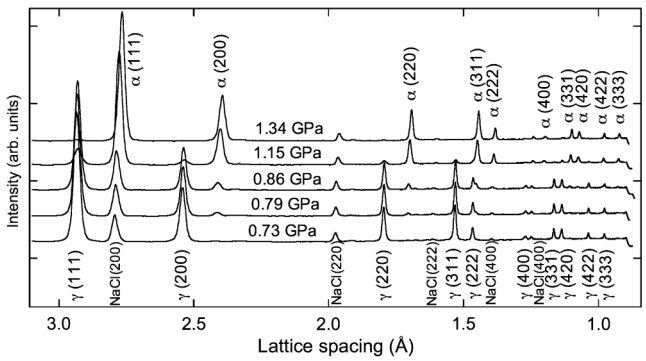

FIG. 2. Angle dispersive diffraction patterns at RT in the vicinity of the VC showing the transition.

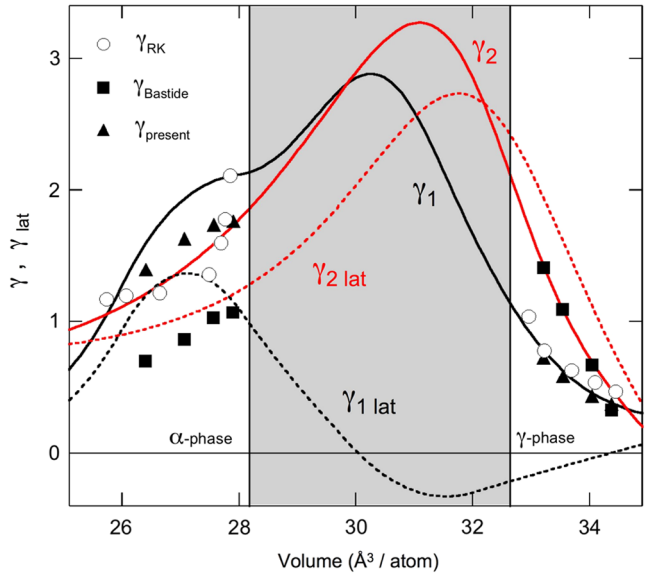

FIG. 3 (color online). Room-temperature thermodynamic $\gamma = V(\partial P/\partial E)_V$ (γ_1, γ_2) and lattice $\gamma_{\rm lat}$ ($\gamma_{1,\rm lat}$, $\gamma_{2,\rm lat}$) Grüneisen parameters as obtained from Eq. (1) in two fits to the pressures (see text). The open circles [32], filled squares [33] and filled triangles (present $V(\partial P/\partial T)_V$ divided by C_V [33]) are experimental results for γ.

approach one another at the volume extremes in Fig. 3. The lattice Grüneisen parameter (dashed curve, $\gamma_{1,\rm lat}$) is seen to be negative on the immediate large-V side of the transition apparently consistent with determinations [12,28] of a decreasing Θ just before the transition. The lattice contribution to the entropy change across the phase transition $3k_B \ln(\Theta_\alpha/\Theta_\gamma)$, however, is only about 2% of the total, since the average $\gamma_{\rm lat}(V)$ is small over the two-phase region in the equivalent expression $3k_B \int dV \gamma_{\rm lat}(V)/V$. This agrees with measurements for Ce alloys [29], but apparently not for Ce itself [12]. Note that no assumptions are made about Poisson's ratio in the use of Eq. (1).

Electron-lattice coupling may well play an important role in the Ce transition given a characteristic electronic temperature T_K [27] that is comparable to the lattice Θ on the large-volume side of the VC. Since electronic structure dictates the interatomic force laws, one might expect differing lattice vibrational properties according to whether the $4f$ moments are well screened or not, as reflected crudely in, e.g.,

$$\ln\Theta(V,T) = \ln\theta_\alpha + \ln(\theta_\gamma/\theta_\alpha) S_K(T/T_K)/S_K(\infty). \quad (2)$$

Here $\theta_\alpha(V)$ and $\theta_\gamma(V)$ depend only on volume, and S_K is the entropy counterpart of C_{VK} which approaches 0 for well screened and $\ln(6) = S_K(\infty)$ for unscreened moments.

We find two classes of solutions in fits to the pressures derived from Eq. (1) using Eq. (2), with the first much like that discussed so far (γ_1 and $\gamma_{1,\rm lat}$ in Fig. 3). The second, which fits the pressures to within a standard deviation of 0.09 GPa (not shown) as compared to 0.08 GPa in Fig. 1, is characterized by thermodynamic (solid curve, γ_2) and lattice (dashed curve, $\gamma_{2,\rm lat}$) Grüneisen parameters also shown in Fig. 3. Note that the lattice contribution to the isotherm spacing $(\partial P/\partial T)_V$ is now $3(\gamma_{\rm lat} + T\partial\gamma_{\rm lat}/\partial T)/V$ which like $3\gamma_{\rm lat}(V)/V$ of the first solution is negative on the large-V side of the transition, even though here $\gamma_{\rm lat}(V,T) = -\partial \ln\Theta(V,T)/\partial \ln V$ itself (dashed curve, $\gamma_{2,\rm lat}$) is positive and sizeable there. This may not conflict with ultrasonic measurements [28] of $\Theta(V)$ which as long-wavelength results should simulate a low-T Θ and do indeed agree with the $T = 0$ neutron scattering result of $\Theta_\gamma = 135$ K [30]. A 16 K decrease in Θ_γ on heating to 300 K [30] may then swamp out any hope of estimating $\gamma_{\rm lat}(V, 300\ {\rm K})$ from [28]. Finally, even though there are now also $\partial \ln\Theta/\partial T$ terms in the entropy, the parameters from this second fit to the pressures yield a lattice entropy change across the RT transition of about 50% in agreement with [12] largely because $\gamma_{\rm lat}(V, 300\ {\rm K})$ is now much larger in the two-phase region, leading to a larger value of the integral $3k_B \int dV \gamma_{\rm lat}(V, 300\ {\rm K})/V$ there.

Figure 4 presents our summary of the p-T phase diagram. We see no evidence in the present x-ray diffraction analyses of distortions of the fcc phase which might signal a 2nd order extension of the phase line [17]. On the other hand a minimum in the bulk modulus does persist to higher temperatures, as indicated by the open circle symbols, obtained from derivatives of polynomial fits to the present isotherms (inset). These points appear to be veering

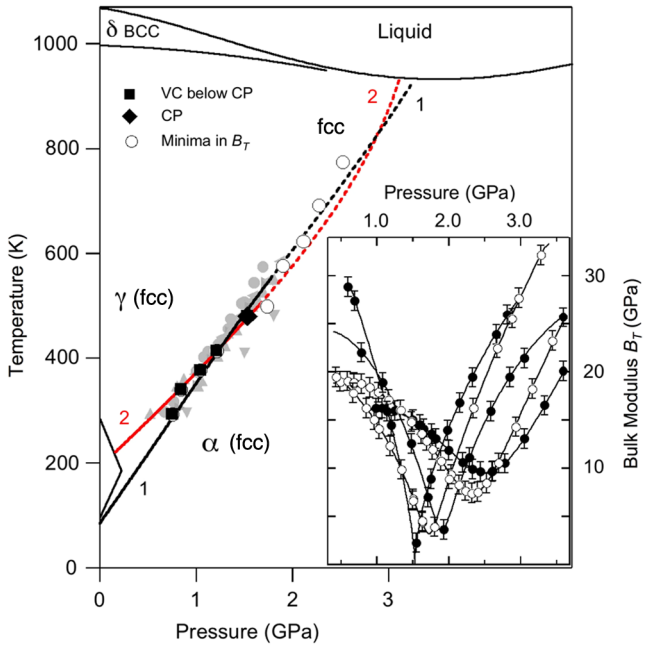

FIG. 4 (color online). Ce phase diagram. Solid black symbols denote present (gray symbols previous [12 ■, 13 ●, 18 ▼, 23 ◀, 24 ▶, 25 ▲]) VC data. The open black circles are bulk modulus B_T minima obtained from the inset showing $B_T(p)$ for $T = 481$, 500, 577, 692, and 775 K. The solid (VC) and dashed (B_T minima) lines are from the two models as labeled.

slightly towards the region of the fcc-δ-phase-liquid triple point rather than the minimum in the melt line. Further experiments at temperatures close to the melt are in progress in order to elucidate the behavior in this region. The phase lines (solid curves, labeled 1,2) and bulk moduli minima (dashed curves, labeled 1,2) corresponding to the two KVC fits are also shown. Note that the transition pressures obtained from the fits are most uncertain where the VC is largest, e.g., <400 K, since those parts of the curves subject to the equal area construction are farthest from and thus least constrained by the data. Both fits exhibit the expected second, low-T CP at negative pressure; i.e., there is no VC at $T = 0$. The lattice vibrations in both fits serve to depress the CP, so that the continued softness in the bulk modulus to higher temperatures is to be expected from the electronic contribution.

In conclusion, this work has presented extensive new high-quality p-V data for the Ce isostructural transition from RT up to 775 K. The data constrains the location of the CP to be $p_c = (1.5 \pm 0.1)$ GPa and $T_c = (480 \pm 10)$ K, resolving previous controversies. There is no evidence of distortions of the fcc structure suggestive of a 2nd order extension of the phase line, although a minimum in the bulk modulus is observed to the highest temperatures investigated. In the first truly quantitative test of the Kondo volume collapse model, it is shown that the data may be fit by the functional forms of this model plus a quasiharmonic treatment of the lattice vibrations to within experimental uncertainties. This simple analysis suggests a profound change in the lattice Grüneisen parameter across the transition which must reflect the differing impact on interatomic forces of the electronic structure with well screened versus unscreened $4f$ moments. It also shows a rich thermal structure associated with the Ce VC which makes apparent the value of improved thermophysical data as presented here in helping to fully understand the nature of this unusual transition.

This work was performed under the auspices of the U.S. Department of Energy by Lawrence Livermore National Laboratory in part under Contract W-7405-Eng-48 and in part under Contract DE-AC52-07NA27344. The x-ray work was performed at beam line 16BMB and 16BMD of the HPCAT at the APS, supported by DOE-BES and DOE-NNSA (CDAC, LLNL, UNLV). We are grateful for experimental help from H. P. Liermann, W. Yang, O. Shebanova (HPCAT), G. W. Lee, and conversations with M. Manley, J. Moriarty, and L. Benedict.

[1] B. Johansson, Philos. Mag. **30**, 469 (1974); B. Johansson, Phys. Rev. B **11**, 2740 (1975).
[2] J. W. Allen and R. M. Martin, Phys. Rev. Lett. **49**, 1106 (1982).
[3] M. Lavagna, C. Lacroix, and M. Cyrot, Phys. Lett. A **90**, 210 (1982).
[4] J. W. Allen and L. Z. Liu, Phys. Rev. B **46**, 5047 (1992).
[5] M. B. Zölfl *et al.*, Phys. Rev. Lett. **87**, 276403 (2001).
[6] K. Held, A. K. McMahan, and R. T. Scalettar, Phys. Rev. Lett. **87**, 276404 (2001).
[7] A. K. McMahan, K. Held, and R. T. Scalettar, Phys. Rev. B **67**, 075108 (2003).
[8] K. Haule, V. Oudovenko, S. Y. Savrasov, and G. Kotliar, Phys. Rev. Lett. **94**, 036401 (2005).
[9] A. K. McMahan, Phys. Rev. B **72**, 115125 (2005).
[10] B. Amadon, S. Biermann, A. Georges, and F. Aryasetiawan, Phys. Rev. Lett. **96**, 066402 (2006).
[11] J. D. Thompson *et al.*, Phys. Rev. Lett. **50**, 1081 (1983).
[12] I.-K. Jeong *et al.*, Phys. Rev. Lett. **92**, 105702 (2004).
[13] R. I. Beecroft and C. A. Swenson, J. Phys. Chem. Solids **15**, 234 (1960).
[14] B. L. Davis and L. H. Adams, J. Phys. Chem. Solids **25**, 379 (1964).
[15] D. A. Young, *Phase Diagrams of The Elements* (University of California Press, Berkeley, 1991), Chap. 14, p. 196.
[16] D. C. Koskenmaki and K. A. Gschneidner, Jr., *Handbook on the Physics and Chemistry of Rare Earths* (North-Holland Publishing Company, Amsterdam, 1978), Chap. 4, p. 337.
[17] G. Eliashberg and H. Capellmann, Pis'ma Zh. Eksp. Teor. Fiz. **67**, 111 (1998) [JETP Lett. **67**, 125 (1998)].
[18] A. Schiwek, F. Porsch, W. B. Holzapfel, High Press. Res. **22**, 407 (2002).
[19] A. P. Hammersley *et al.*, High Press. Res. **14**, 235 (1996).
[20] G. Gu, Y. Vohra, and K. E. Brister, Phys. Rev. B **52**, 9107 (1995).
[21] J. S. Olsen, L. Gerward, U. Benedict, and J.-P. Itié, Physica (Amsterdam) **133B+C**, 129 (1985).
[22] L. D. Landau and E. M. Lifschitz, *Statistical Physics, Course of Theoretical Physics* (Pergamon Press Ltd., London, 1958), Vol. 5, p. 259.
[23] A. R. Kutsar, Dokl. Akad. Nauk SSSR **245**, 1360 (1979) [Sov. Phys. Dokl. **24**, 292 (1979)].
[24] A. Jayaraman, Phys. Rev. **137**, A179 (1965).
[25] E. G. Poniatovskii, Dokl. Akad. Nauk SSSR **120**, 1021 (1959) [Sov. Phys. Dokl. **3**, 498 (1959)].
[26] L. D. Livshitz, Yu. S. Genshaft, and V. K. Markov, Zh. Eksp. Teor. Fiz. **43**, 1262 (1962) [Sov. Phys. JETP **16**, 894 (1963)].
[27] The fit in Fig. 1 yields $T_K = 2172$, 1034, 106, and 12 K for $V = 25$, 28.2 (α), 32.6 (γ), and 35 Å^3/atom. These values roughly scale with the C_{VK} maximum, here $T/T_K = 0.57$.
[28] F. F. Voronov, L. F. Vereschagin, and V. A. Goncharova, Sov. Phys. Dokl. **135**, 1280 (1960).
[29] M. E. Manley *et al.*, Phys. Rev. B **67**, 014103 (2003).
[30] C. Stassis *et al.*, Phys. Rev. B **19**, 5746 (1979).
[31] F. Birch, J. Geophys. Res. **91**, 4949 (1986).
[32] J. Ramakrishnan and G. C. Kennedy, J. Appl. Phys. **51**, 2586 (1980).
[33] J.-P. Bastide, C. Loriers-Susse, H. Massat, and B. Coqblin, High Temp. High Press. **10**, 427 (1978). Table I gives the thermal expansion α, the bulk modulus B_T (K_T), the specific heat C_V ($C_V{}^{\mathrm{res}} + C_V{}^{\mathrm{el}}$), and thus $\gamma = \alpha B_T V / C_V$.